



Our interest lies in the design of chemosensors for metals of biological interest.<sup>12</sup> Chemosensors are molecules that translate chemical information, such as the presence of a certain metal ion, into an analytically useful signal.<sup>13</sup> Thus, a molecular recognition group is coupled to a reporter group, and an efficient signal transduction between these two moieties has to take place. In squaric acid **1**, two vinylogous acid moieties are “cross-conjugated”, enabling a tight electronic coupling between them. This feature makes the squaric acid moiety attractive as a linker between a metal recognition site and the reporter group in the construction of chemosensors. A further advantage is conceivably derived from involving the squarate oxygens in the metal binding. Early reports on the coordination chemistry of the squarate dianion proposed an  $\eta^2$ -coordination mode (**1M**);<sup>14</sup> however, later papers showed that the bite angle imposed by the cyclobutene framework is too large to sustain this coordination mode with first and second row transition metals (bite distance of 3.3 vs 2.6 Å for the chelating anion oxalate). Instead, only  $\eta^1$ -coordination such as the 1,2-bismonodentate coordination mode (**1M<sub>2</sub>**) is observed.<sup>15</sup> Monodentate binding is less strong and specific than chelate formation, and therefore to design a metal-specific sensor incorporating a squaric acid moiety, we had to redesign the metal binding motif.

The anions of hydroxamic acids are known to form chelates with iron(III) with high specificity,<sup>16</sup> and these iron(III) hydroxamate complexes can possess great thermodynamic stability. This property is utilized by many microorganisms to sequester iron by secreting hydroxamic acid-based siderophores.<sup>17,18</sup> The squaric acid *N*-hydroxylamide ester derivative **5** is a vinylogous hydroxamic acid (Scheme 1). Molecular modeling suggests that the anion of this hydroxamic acid analogue possesses the proper metric requirements for chelation, and it forms a six-membered metallacycle **5M** (bite distance between the oxygens 2.8 Å).<sup>19</sup> A range of *N*-hydroxylamide methyl-esters of type **5** were first reported by Zinner and Grünefeld and tested for their iron(III)-binding properties.<sup>20</sup> Surprisingly, however, chelation was only observed under anhydrous conditions in aprotic solvents, suggesting hydrolytic lability (i.e., low stability) for these complexes. The authors also prepared the corresponding *N*-hydroxylamide amides **6** but did not report on their chelation behavior, and they reported an unexpected inability to prepare squarate bis-*N*-hydroxylamides **7**.

In our search for novel ways to bring a hydroxamate-type chelating moiety into close electronic contact with, for instance, a fluorophore for the construction of chemosensors for iron(III), we decided to reinvestigate the synthesis and chelation properties of the *N*-hydroxylamide esters and amides. In this process, we fine-tuned and expanded the synthetic methodology toward **5** and **6** and related compounds. We unveiled the reason bishydroxamates **7** could not be prepared by nucleophilic displacement of diester **2**. <sup>13</sup>C NMR spectroscopy of the squaric acid derivatives gains a particularly important role in their characterization because of the paucity of nonexchangeable or diagnostic protons in these structures, but the carbons of the cyclobutenedione framework of many derivatives were characterized by unusually long <sup>13</sup>C relaxation times. We determined the spin–lattice relaxation time *T*<sub>1</sub> of the squarate derivatives. This investigation also provided spectroscopic evidence for the degree by which resonance structures determine their differing coordination properties. The results of the synthesis and spectroscopic and structural investigations of *N*-alkylhydroxylamide squarate esters **5**, amides **6**, and related compounds are reported here.

## Results and Discussion

**Synthesis of Squaric Acid Hydroxamate Esters **5** and Amides **6**.** The ultimate starting material for all our syntheses was 3,4-dimethoxycyclobut-3-ene-1,2-dione (**2a**), prepared from disilver(I) squarate and methyl iodide following a procedure similar to a Williamson ether synthesis.<sup>21</sup> We chose the solid dimethyl ester **2a** over

(7) (a) Tomas, S.; Rotger, M. C.; Gonzalez, J. F.; Deya, P. M.; Ballester, P.; Costa, A. *Tetrahedron Lett.* **1995**, *36*, 2523–2526. (b) Prohens, R.; Tomas, S.; Morey, J.; Deya, P. M.; Ballester, P.; Costa, A. *Tetrahedron Lett.* **1998**, *39*, 1063–1066. (c) Tomas, S.; Prohens, R.; Deslongchamps, G.; Ballester, P.; Costa, A. *Angew. Chem., Int. Ed.* **1999**, *38*, 2208–2211. (d) Prohens, R.; Martorell, G.; Ballester, P.; Costa, A. *Chem. Commun.* **2001**, 1456–1457. (e) Prohens, R.; Rotger, M. C.; Piña, M. N.; Deya, P. M.; Morey, J.; Ballester, P.; Costa, A. *Tetrahedron Lett.* **2001**, *42*, 4933–4936.

(8) Tietze, L. F.; Arlt, M.; Beller, M.; Glusenkamp, K. H.; Jahde, E.; Rajewsky, M. F. *Chem. Ber.* **1991**, *124*, 1215–1221.

(9) (a) Gardner, S. H.; Freyschmidt-paul, P.; Hoffman, R.; Sundberg, J. P.; Happle, R.; Nigel, J.; Tobin, D. J. *Eur. J. Dermatol.* **2000**, *10*, 443–450. (b) Freyschmidt-paul, P.; Sundberg, J. P.; Happle, R.; McElwee, K. J.; Metz, S.; Boggess, D.; Hoffman, R. J. *Investigative Dermatol.* **1999**, *113*, 61–68. (c) Kazumasa, M.; Motonobu, N.; Miyako, N.; Tatsuo, K.; Yoshiki, M. *J. Dermatol.* **2002**, *29*, 661–664. (d) Silverberg, N. B.; Lim, J. K.; Paller, A. S.; Mancini, A. J. *J. Am. Acad. Dermatol.* **2000**, *42*, 803–808.

(10) (a) Bang-Andersen, B.; Ahmadian, H.; Lenz, S. M.; Stensbøl, T. B.; Madsen, U.; Bøgesø, K. P.; Krosgaard-Larsen, P. *J. Med. Chem.* **2000**, *43*, 4910–4918. (b) Butera, J. A.; Antane, M. M.; Antane, S. A.; Angentieri, T. M.; Freedon, C.; Graceffa, R. F.; Hirth, B. H.; Jenkins, D.; Lennox, J. R.; Matelan, E.; Norton, N. W.; Quagliato, D.; Sheldon, J. H.; Spinelli, W.; Warg, D.; Wojdan, A.; Woods, M. *J. Med. Chem.* **2000**, *43*, 1187–1202. (c) Gilbert, A. M.; Antane, M. M.; Angentieri, T. M.; Butera, J. A.; Francisco, G. D.; Freedon, C.; Gundersen, E. G.; Graceffa, R. F.; Herbst, D.; Hirth, B. H.; Lennox, J. R.; McFarlane, G.; Norton, N. W.; Quagliato, D.; Sheldon, J. H.; Warg, D.; Wojdan, A.; Woods, M. *J. Med. Chem.* **2000**, *43*, 1203–1214.

(11) Zhang, J.; Zhou, H.-B.; Lü, S.-M.; Luo, M.-M.; Xie, R. G.; Choi, M. C. K.; Zhou, Z.-Y.; Chan, S. C.; Yang, T.-K. *Tetrahedron: Asymmetry* **2001**, *12*, 1907–1912.

(12) Lim, N. C.; Yao, L.; Freake, H. C.; Brückner, C. *Bioorg. Med. Chem. Lett.* **2003**, *13/14*, 2251–2254.

(13) de Silva, A. P.; Gunaratne, H. Q. N.; Gunlaugsson, T.; Huxley, A. J. M.; McCoy, C. P.; Rademacher, J. T.; Rice, T. E. *Chem. Rev.* **1997**, *97*, 1515–1566.

(14) (a) West, R.; Niu, H. Y. *J. Am. Chem. Soc.* **1963**, *85*, 2589–2590. (b) Ludi, A.; Schindler, P. *Angew. Chem., Int. Ed. Engl.* **1968**, *7*, 638.

(15) See e.g.: (a) Habenschuss, M.; Gerstein, B. C. *J. Chem. Phys.* **1973**, *61*, 852–860. (b) Weiss, A.; Riegler, E.; Robl, C. *Z. Naturforsch., B: Chem. Sci.* **1986**, *41*, 1329–1332. (c) Weiss, A.; Riegler, E.; Robl, C. *Z. Naturforsch., B: Chem. Sci.* **1986**, *41*, 1332–1336. (d) Solans, X.; Aguilo, M.; Gleizes, A.; Faus, J.; Julve, M.; Verdager, M. *Inorg. Chem.* **1990**, *29*, 775–784. (e) Khan, M. I.; Chang, Y.-D.; Chen, Q.; Salta, J.; Lee, Y.-S.; O'Connor, C. J.; Zubietta, J. *Inorg. Chem.* **1994**, *33*, 6340–6350. (f) Hilbers, M.; Meiwald, M.; Mattes, R. *Z. Naturforsch., B: Chem. Sci.* **1996**, *51*, 57–67.

(16) Mehrota, R. C. In *Comprehensive Coordination Chemistry*; Wilkinson, G. G., R. D., McCleverty, J. A., Eds.; Pergamon Press: Oxford, 1987; Vol. 2, pp 505–514.

(17) Raymond, K. N.; Müller, G.; Matzanke, B. F. *Topics Curr. Chem.* **1984**, *123*, 49–102.

(18) Miller, M. J. *Chem. Rev.* **1989**, *89*, 1563–1579.

(19) *Quantum CACHE 4.9, MM3 force field*; Fujitsu Limited, 2002.

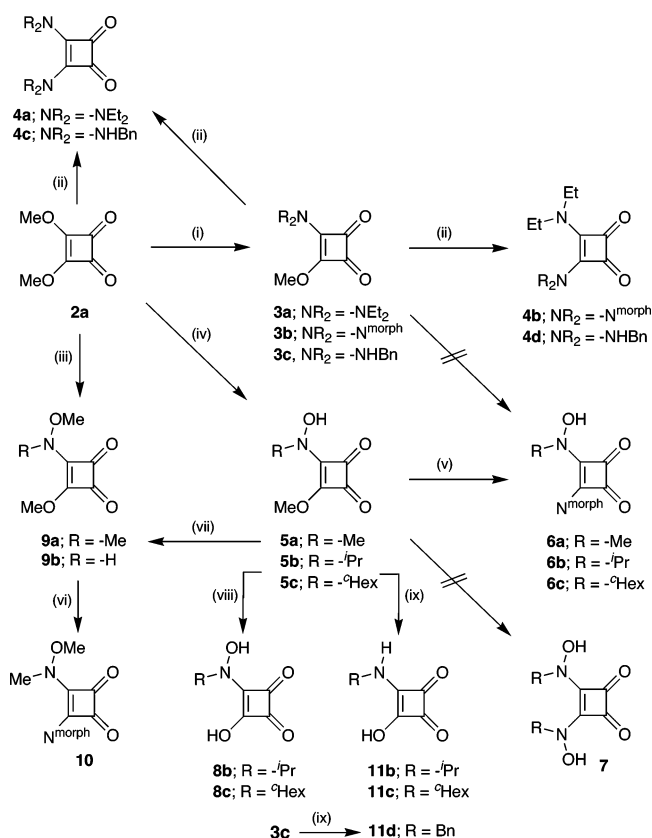
(20) Zinner, G.; Grünefeld, J. *Arch. Pharm. (Weinheim, Ger.)* **1985**, *318*, 977–983.

(21) (a) Cohen, S.; Cohen, S. G. *J. Am. Chem. Soc.* **1966**, *88*, 1533–1536. (b) Alternative methods for the synthesis of squarate esters are available; see e.g.: Liu, H.; Tomooka, C. S.; Moore, H. W. *Synth. Commun.* **1997**, *27*, 2177–2180.

the more commonly used liquid diethyl ester because it is readily prepared in high purity and is much less prone to hydrolytic degradation. Parallel to the reactivity of the diethyl ester, dimethyl ester **2a** reacted with a slight excess (~1.1 equiv) of *N*-alkylamine in MeOH under reflux conditions to afford the corresponding *N*-alkylamide methylesters squarates **3a–c**.<sup>5</sup> Reaction of these *N*-alkylamide methylesters with a molar excess of *N*-alkylamine produced the bis-*N*-alkylamides with identical (**4a**, **4c**) or mixed (**4b**, **4d**) *N*-alkyl substituents.<sup>8</sup> The preparation of the known (**3a**,<sup>22</sup> **4a**, **4c**<sup>23</sup>) or novel (**3b**, **3c**, **4b**, **4d**) compounds serves as a reference point for the synthesis of the *N*-hydroxylamide derivatives.

In analogy to the preparation of the monoamide monoesters **3** upon treatment of dimethyl squarate **2a** with 1.1 equiv of free base *N*-alkylhydroxylamines in MeOH at ambient temperature, the corresponding *N*-alkylhydroxylamide methylester squarates **5a–c** were produced.<sup>20</sup> Conversion of **5a–c** to the corresponding *N*-alkylhydroxylamide *N*-morpholinamide squarates **6a–c** was achieved by addition of 2 equiv of morpholine, also in MeOH and at ambient temperature. The inverse reaction, i.e., the preparation of the compounds **6a–c** by reaction of morpholinamide methylester squarate (**3b**) with an *N*-alkylhydroxylamine was not possible, even when using a large excess of hydroxylamine under forcing conditions (reflux in MeOH or EtOH for 48 h, with or without the addition of KOH or Et<sub>3</sub>N). The starting materials were recovered quantitatively. Our results are in accordance with the report by Zinner and Grünefeld.<sup>20</sup> This finding suggests a different mechanism for the formation of the *N*-alkylhydroxylamide ester squarates from squarate esters and hydroxylamines than implied by the overall nucleophilic substitution reaction. A possible mechanism for this reaction is discussed below.

Upon stirring of the ester hydroxamate **5** in water at room temperature, the slow formation of the expected hydrolysis products **8** was observed by +ESI-MS (e.g., for **8b**, *m/z* = 172, corresponding to MH<sup>+</sup>). However, even after 1 week of reaction time, only partial conversion of the starting material took place, despite the fact that an autocatalytic reaction is expected to occur, as acids **8** are expected to be strong acids (cf. to the *pK*<sub>1</sub> and *pK*<sub>2</sub> of **1** of 0.5 and 3.5, respectively).<sup>4</sup> Moreover, the *N*-dehydroxylated species **11** was formed over time (e.g., for **11b**, *m/z* = 156, corresponding to MH<sup>+</sup>). Hydrolysis of **5** under acidic (1.2 M aq HCl) or basic (1 M aq KOH) conditions resulted in the formation of **11** in quantitative yields. The elimination of the hydroxyl group from hydroxamic acids has been previously observed.<sup>24</sup> Thus, we were not able to prepare the *N*-hydroxylamide acids **8** in pure form. The amide acids **11** could also be prepared independently by hydrolysis of the ester amides **3**. For instance, acid-catalyzed hydrolysis of ester amide **3c** provided **11d** in good yields.

SCHEME 2<sup>a</sup>

<sup>a</sup> Reaction Conditions: (i) 1.0 equiv of HNR<sub>2</sub>/MeOH, Δ;<sup>5</sup> (ii) molar excess of HNR<sub>2</sub>/MeOH, Δ;<sup>23</sup> (iii) 1.7 equiv of HNROMe/MeOH, 25 °C;<sup>20</sup> (iv) 1.1 equiv of HNROH/MeOH, 25 °C;<sup>20</sup> (v) 2 equiv morpholine/MeOH, 25 °C; (vi) 5 equiv of morpholine/MeOH, 25 °C; (vii) CH<sub>2</sub>N<sub>2</sub>/Et<sub>2</sub>O, 25 °C; (viii) H<sub>2</sub>O, 25 °C; (ix) 1.2 M aq HCl or 1.0 M aq KOH.

The *O*-alkylated species **9** and **10** are expected to be incapable of binding iron in the hydroxamate *O,O*-bidentate fashion. They are thus intended to serve in detailed binding studies as the nonspecific metal binding analogues to hydroxamates **5** and **6**. *N*-Methylhydroxylamide ester **5a** can be alkylated with diazomethane to provide *N,O*-dimethylhydroxylamide methylester **9a**. A more convenient way to prepare this material, however, is by reaction of dimethylsquarate **2a** with *O*-alkylhydroxylamines.<sup>20</sup> The *O*-methylhydroxylamide methylester **9a** can be converted in good yield to the corresponding *O*-methylhydroxylamide *N*-morpholinamide **10** by reaction with a 5-fold molar excess of morpholine.

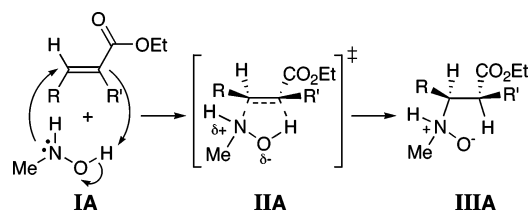
**Mechanism of Formation of the Squaric Acid Hydroxamates.** As shown, squarate dimethyl ester **2a** readily reacts with *N*-alkylhydroxylamines to provide the corresponding *N*-alkylhydroxylamide methylester squarates **5a–c**. Treatment of **5a–c** with *N*-alkylhydroxylamines, however, does not lead to the formation of the bis-*N*-alkylhydroxylamides **7** under any condition tested (Scheme 2).<sup>20</sup> On the other hand, reaction of **5** with 1–3 equiv *N*-alkylamines affords the corresponding *N*-alkylhydroxylamide alkylamide squarates **6** in good yields at ambient temperature within 1 h. This is surprising in light of the reported higher nucleophilicity of *N*-hydroxylamines toward sp<sup>2</sup> centers as compared to *N*-alkyl-

(22) Hall, L. A.; Williams, D. J.; Menzer, S.; White, A. J. P. *Inorg. Chem.* **1997**, *36*, 3096–3101.

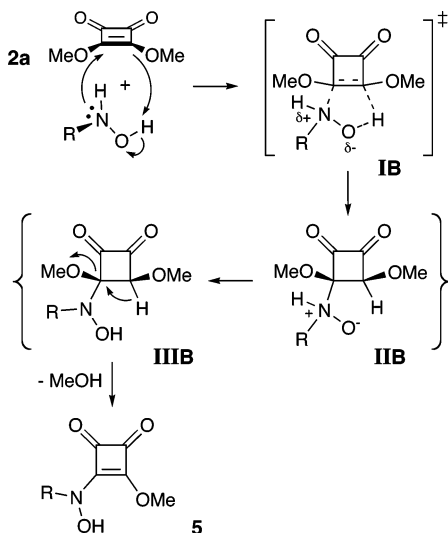
(23) Thorpe, J. E. *J. Chem. Soc. B* **1968**, 435–436.

(24) For examples of the dehydroxylation of hydroxamates under a variety of reaction conditions, see e.g.: (a) Surman, M. D.; Mulvihill, M. J.; Miller, M. J. *Tetrahedron Lett.* **2002**, *43*, 1131–1134. (b) Quadrelli, P.; Campari, G.; Mella, M.; Caramella, P. *Tetrahedron Lett.* **2000**, *41*, 2019–2022. (c) Ayyangar, N. R.; Kalkote, U. R.; Nikrad, P. V. *Indian J. Chem., Sect. B* **1983**, *22*, 872–877. (d) Mattingly, P. G.; Miller, M. J. *J. Org. Chem.* **1980**, *45*, 410–415. (e) Birchall, J. D.; Glidewell, C. *J. Chem. Soc., Dalton Trans.* **1978**, 604–607.



SCHEME 3<sup>26</sup>

## SCHEME 4

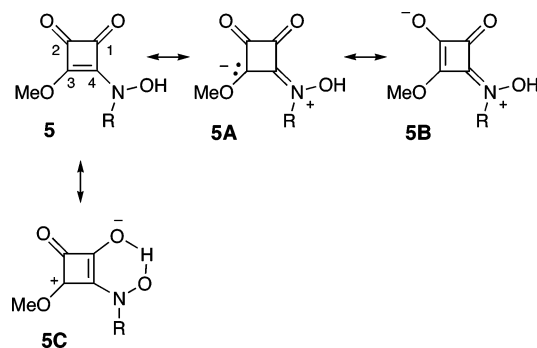


amines.<sup>25,26</sup> Similarly, formation of the squarate diamides **4** by nucleophilic substitution of the squarate ester amides **3** is possible, while the analogous reaction of **3** with *N*-hydroxylamines fails to provide any product.<sup>20</sup>

These findings suggest that *N*-alkylhydroxylamines react with squarate esters by a different mechanism than the expected nucleophilic substitution pathway of regular *N*-alkylamines. Precedents for the varying reactivity of the two nitrogen-based nucleophiles are known. For instance, conjugate addition of hydroxylamines to  $\alpha,\beta$ -unsaturated esters proceeds smoothly, but no reaction with the corresponding *O*-alkylhydroxylamines and alkylamines is observed.<sup>27</sup> To explain this finding, a concerted mechanism for the addition was proposed, assigning a key role to the hydroxyl hydrogen (Scheme 3).<sup>26,27</sup> Nucleophilic attack by the nitrogen lone pair to the alk-enone **1A** generates the cyclic five-membered ring transition state **IIA**. This transition state resembles that of a [3 + 2] dipolar cycloaddition reaction or retro-Cope elimination reaction. Its collapse generates the species **IIIA**, and a rapid N-to-O proton shift then provides the final product.

A similar mechanism can be hypothesized to explain the formation of *N*-alkylhydroxylamide methylesters **5** by reaction of a squarate diester **2** with a *N*-alkylhydroxylamine (Scheme 4). Upon nucleophilic attack of *N*-alkylhydroxylamine to dimethyl squarate **2a**, the five-membered transition state **IB** is formed. Collapse of this

## SCHEME 5



transition state provides **IIB**. Formal N-to-O proton transfer and subsequent anti elimination of methanol (**IIB**) leads to the formation of *N*-alkylhydroxylamide methylester squarate **5**. All steps involved are highly suggestive of a concerted mechanism, making a collapse of **IB** and direct formation of the final product likely.

Why, then, is the failure to form bis-*N*-hydroxylamide squarates observed? Considering the amide character of **5** with its canonical structures **5A** and **5B** (Scheme 5), nucleophilic attack at C3 and subsequent formation of the five-membered transition state is unfavorable due to the mismatched polarity of **5A** and **5B** and the nucleophile. Resonance structure **5C** is favored by the expression of a H-bond between the hydroxylamide hydrogen and the adjacent carbonyl group, and the limiting resonance structure is represented by **5C**. Though this structure polarizes C3 toward nucleophilic attack, the C3–C4 bond no longer possesses any double-bond character. However, a double bond at this position is required for the 3 + 2-type mechanism to take place. On the other hand, the polarity of C3 allows a simple nucleophilic substitution mechanism by an alkylamine to occur. This hypothesis is consistent with the observed reactivity of **5**. Further spectroscopic and structural evidence for the polarity and limiting resonance structures evoked are presented below.

**Spectroscopic Comparison of the Hydroxamate Squarates and Hydroxamic Acids.** Formally, squarate esters **2** are not esters, i.e., they do not contain an ester moiety. Likewise, hydroxamate squarates **5** and **6** are not true hydroxamic acids. They are best described as vinyllogous hydroxamic acids. Furthermore, and in stark contrast to hydroxamic acids, the *N*-hydroxyl group is not in conjugation with its *adjacent* carbonyl group but is instead in conjugation with the carbonyl group *opposite* to it. This peculiarity has consequences when considering the bond arrangements upon binding of a metal as compared to those found in a hydroxamate metal complex (Figure 1). The O,O-donor set in an [hydroxamate]M complex is provided by a deprotonated *N*-hydroxide and an amide carbonyl (**I**). The limiting resonance structure **II** expresses the amide character of this carbonyl group; the existence of resonance structures is responsible for the tight binding of the metal. To illustrate the profound differences in the bonding arrangement found in a hydroxamate squarate metal complex, consider the resonance structures **I** and **II** of the chelate **11M**. Although the O,O-donor set for the metal is also provided by a *N*-hydroxide and its adjacent carbonyl group, the carbonyl group is *not* in conjugation with the amide nitrogen

(25) Collis, M. P.; Hockless, D. C. R.; Perlmutter, P. *Tetrahedron Lett.* **1995**, 36, 7133–7136.

(26) Niu, D.; Zhao, K. *J. Am. Chem. Soc.* **1999**, 121, 2456–2459.

(27) (a) Fountain, K. R.; Erwin, R.; Early, T.; Kehl, H. *Tetrahedron Lett.* **1975**, 35, 3027–3030. (b) Moglioni, A. G.; Muray, E.; Castillo, J. A.; Alvarez-Larena, A.; Moltrasio, G. Y.; Branchadell, V.; Ortuño, R. M. *J. Org. Chem.* **2002**, 67, 2402–2410.

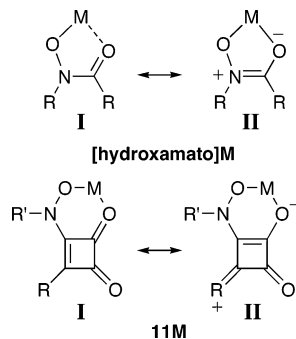


**FIGURE 1.** Resonance structures of metal hydroxamates as compared to metal hydroxamate squarate **11M**.

of the *N*-hydroxide. Therefore, the donor capability of this carbonyl oxygen is largely determined by the nature of the fourth ring substituent, here the group  $-R$ . In hydroxamate ester squarates such as **5**, this carbonyl has ester carbonyl character, and consequently, it is a comparably bad donor. In the hydroxamate amide squarates **6**, this carbonyl has amide character and, hence, carries a much higher partial negative charge and, thus, is a better donor. This interpretation is the key to understanding the largely differing iron binding properties of the *N*-hydroxamate esters and amides. Further, this interpretation also predicts that the *N*-hydroxamate acids **8**, which carry a large negative charge on the oxygen, should be excellent chelators. We are currently seeking an alternative pathway toward their synthesis.

**$^{13}\text{C}$  NMR Spectroscopy.** Our initial efforts to characterize the squaric acid derivatives by  $\{^1\text{H}\}^{13}\text{C}$  NMR spectroscopy using standard 1–2 s delay times were thwarted by the inability to detect all of the expected cyclobutenedione framework carbons in many of the derivatives studied. The problem was found to lie in long spin-lattice relaxation times ( $T_1$ ). This led to a systematic investigation of the  $^{13}\text{C}$   $T_1$  of these derivatives. The results are tabulated in Table 2.

Across the table, the chemical shifts of the carbons vary only slightly and in predictive ways: each (vinyllogous) ester moiety is characterized by a carbonyl carbon shift between  $\sim 185$ – $190$  ppm and the corresponding  $\beta$ -carbon at  $\sim 175$ – $177$  ppm (**2**, **3**, **5**, and **9**). By contrast, each (vinyllogous) amide moiety resonates at  $\sim 179$ – $184$  and  $164$ – $170$  ppm (**4**, **5**, **6**, **9**, and **10**), respectively. Each (vinyllogous) acid functionality exhibits a signal between  $186$  and  $190$  ppm (**1** and **11**). These shifts can be interpreted in light of the predominant resonance structures of the vinyllogous ester, amide, and acid functionalities.

In  $\text{DMSO}-d_6$ , the  $T_1$  values range from  $0.6$  s in squaric acid to well over  $20$  s in **2a**, **3a**, **4d**, **9a**, and **10**. Some trends in the relaxation times can be traced. Each compound class is characterized by a specific range of  $T_1$ . Thus, the compound classes can be ranked according to increasing  $T_1$ : squaric acid **1** (less than  $1$  s) < hydroxamate amides **6** ( $2$ – $3$  s) < amide acids **11** ( $8$ – $10$  s) < hydroxamate esters **5** ( $8$ – $12$  s) < diamide **4** ( $10$ – $15$  s) < ester amide **3a** ( $12$ – $20$  s)  $\approx$  diester **2a** ( $13$ – $26$  s). Again, the ranking of these compound classes reflects their ability to undergo resonance stabilization. Two examples may serve to illustrate this. Both hydroxamate amides **6** and hydroxamate esters **5** can undergo reso-

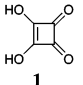
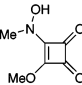
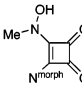
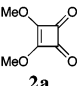
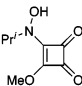
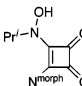
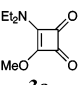
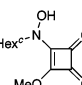
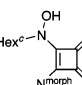
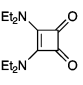
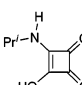
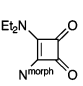
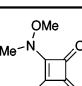
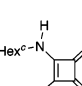
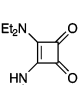
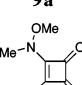
nance stabilization by forming hydrogen bonds, whereas amides **6** are much better H-acceptors. If the hydrogen bond donor group is methylated (**9a** from ester hydroxamate **5a** or **10** from amide hydroxamate **6a**), the relaxation times increase dramatically (cf. **9a** ( $11$ – $20$  s) to **5a** ( $9$ – $13$  s); cf. **10** ( $9$   $\rightarrow$   $20$  s) to **6a** ( $6$ – $11$  s)) and fall into the class of the corresponding ester amides **3** or diamides **4**, respectively.

Why does a greater ability to delocalize charge efficiently reduce the spin–lattice relaxation times in these small molecules? In spin–lattice relaxation, the excited nuclei transfer their excitation energy to their environment. They do so via interaction of their magnetic vectors with fluctuating local fields of sufficient strength and a fluctuation frequency of the order of the Larmor frequency of the nuclear spin type.<sup>28</sup> The efficiency of this process is reflected in the measured relaxation time  $T_1$ . A short  $T_1$  corresponds to an efficient relaxation or a long correlation time between nuclei. Depending upon the atomic and electronic environment of a nucleus in a molecule and the motion of that molecule, there are four potential mechanisms contributing to spin–lattice relaxation of the nucleus: chemical shift anisotropy (CSA), scalar coupling (SC), spin rotation (SR), and dipole–dipole interaction (DD).<sup>28</sup> DD is unlikely to be the dominant relaxation mechanism in the squarates, since this relaxation mechanism is dominant in C–H bonds and no such bonds exist in the squarate core. Likewise, SR and SC are not the dominant mechanisms, as all compounds are of comparable shape and size and have no large  $J$  couplings. This excludes dramatically different spinning rates, anisotropies in their spinning motions, or different segmental motions. This leaves CSA, which is the modulation of the anisotropic shielding by a nuclear or electron tensor within the molecule. The delocalization and charge separation in the cyclobutenedione framework aids relaxation in the hydroxamate derivatives. Thus, we believe it is the CSA term that is primarily responsible for the observed modulation of the spin–lattice relaxation times. The different degrees to which resonance structures are expressed in the squarate esters and amides change the dipole moments and polarizability of all bonds of the framework and those attached to it. This, in turn, changes the number of CSA interactions, which can contribute to an efficient relaxation of the  $^{13}\text{C}$  excitation energy to their environment. Nonetheless, some influence of the SC term to the  $T_1$  modulation cannot be ruled out since the cyclobutenedione framework in the compounds considered is decorated with either four oxygens, three oxygens, and one nitrogen or two elements of each. This alteration results in different, albeit small, scalar coupling terms.

Qualitatively, this interpretation is supported by the trends observed in the  $\nu_{\text{O-H}}$  and  $\nu_{\text{C=O}}$  stretching frequencies in the vibrational spectra of the derivatives. For instance, the  $\nu_{\text{C=O}}$  band of the vinyllogous ester moieties is found at  $\sim 1800$   $\text{cm}^{-1}$  throughout all compounds (see **2**, **3**, **5**, and **9**). As expected, the amide  $\nu_{\text{C=O}}$  band is found at lower wavenumbers ( $1700$ – $1660$   $\text{cm}^{-1}$ ) whereby their position is dependent on the particular compound class. Ester amides such as **3**, **5**, and **9** are found at the upper

(28) Breitmaier, E.; Spohn, K.-H.; Berger, S. *Angew. Chem., Int. Ed. Engl.* **1975**, *14*, 144–159.

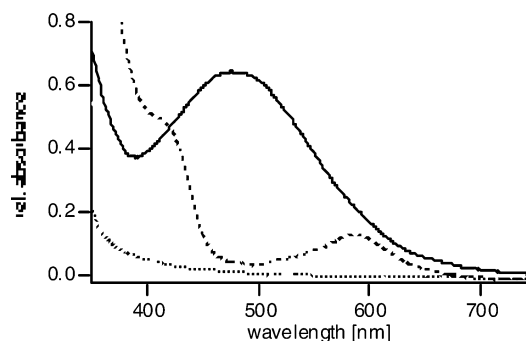
**TABLE 1.**  $^{13}\text{C}$  NMR Shifts (100 MHz,  $\text{DMSO}-d_6$ , 27 °C) and Associated Spin–Lattice Relaxation Times  $T_1$  for the Carbons of the Cyclobutenedione Framework of Select Squarates<sup>a</sup>

Compound	$\delta$ [ppm]	$T_1$ [s]	Compound	$\delta$ [ppm]	$T_1$ [s]	Compound	$\delta$ [ppm]	$T_1$ [s]
 <b>1</b>	191.8	0.6	 <b>5a</b>	186.0 179.5 175.0 167.8	11.7 12.9 8.8 9.4	 <b>6a</b>	181.0 179.2 165.8 164.9	8.6 11.6 6.2 5.7
 <b>2a</b>	190.0 184.7	35.4 26.1	 <b>5b</b>	185.8 180.0 175.5 168.2	11.6 13.0 19.1 9.8	 <b>6b</b>	181.3 179.2 166.2 165.1	2.0 2.5 2.0 2.1
 <b>3a</b>	189.5 181.9 177.1 171.2	16.7 21.4 18.3 12.5	 <b>5c</b>	186.0 180.1 175.7 168.3	9.3 10.3 9.9 8.4	 <b>6c</b>	181.5 179.2 166.3 165.1	3.1 3.4 2.5 2.6
 <b>4a</b>	183.9 169.4	14.9 11.1				 <b>11b</b>	187.0 (br) <sup>c</sup> 186.1 184.7 (br) <sup>c</sup> 174.7	(9.7) <sup>c</sup> 9.7 (9.7) <sup>c</sup> 5.1
 <b>4b</b>	184.4 183.6 169.0 168.0	15.0 13.5 9.4 10.2	 <b>9a</b>	185.3 181.0 175.9 169.0	16.0 18.0 20.4 11.4	 <b>11c</b>	187.0 (br) <sup>c</sup> 186.2 184.7 (br) <sup>c</sup> 174.9	(8.5) <sup>c</sup> 8.5 (8.5) <sup>c</sup> 4.2
 <b>4d</b>	183.2 182.3 167.0 167.5	27.4 15.2 6.1 6.4	 <b>10</b>	182.5 179.3 166.7 164.4	8.7 >20 <sup>b</sup> 21.7 9.2			

<sup>a</sup>  $T_1$  data was acquired using a standard inversion recovery sequence with proton decoupling using a QNP probe; delay between scans was set at approximately 10 s with variable delays ranging from 0.5 to 60 s. For each delay, 400–512 scans were acquired. For a full listing of the  $^1\text{H}$  and  $^{13}\text{C}$  NMR shifts, see Experimental Section. <sup>b</sup> Insufficient number of data points collected to determine the  $T_1$  with greater precision. <sup>c</sup> Broadened signals for **11b–c** suggest exchange phenomena that may diminish the validity of the  $T_1$  determinations; see Supporting Information for the  $^{13}\text{C}$  spectra of these novel squaric acid monoamides.

range, while those of the diamides **4** and **10** and the hydroxylamide amides **6** are shifted down to 1670–1660  $\text{cm}^{-1}$ . In the *N*-hydroxylamide amide **6a**, a  $\nu_{\text{C=O}}$  band at 1660  $\text{cm}^{-1}$  is observed. O-Methylation breaks the possible H-bond and the  $\nu_{\text{C=O}}$  band shifts to 1675  $\text{cm}^{-1}$ . However, a comprehensive interpretation of the IR data is made impossible by the inability to unambiguously assign all peaks above 1500  $\text{cm}^{-1}$ .

**Preliminary Metal Binding Studies.** The red-purple iron(III) complexes of hydroxamates are characterized by a relatively strong ( $\epsilon \approx 3000$ ) and broad (half-height width of  $\sim 200$  nm) ligand-to-metal charge-transfer band centered at around 500 nm.<sup>29</sup> Figure 2 shows the UV–vis spectra of aqueous solutions of **5b** and **6b** in the presence of 1/3 mol ratio  $\text{Fe}^{3+}$  in comparison to the spectrum of the tris[*N*-tolylbenzhydroxamate]iron(III) complex. Consistent with the report by Zinner and Grünefeld,<sup>20</sup> squaric acid *N*-hydroxylamide ester **5b** provides no indication for metal binding. However, the corresponding amide **6b** exhibits a UV–vis band upon treatment with iron(III) (Figure 2). This indicates a binding event but does not allow a clear interpretation of the binding mode, especially as the green color pales over time. A detailed investigation of the coordination interaction is underway. This experiment, however,

**FIGURE 2.** UV–vis spectra of **5b** (···), **6b** (---), and *N*-tolylbenzhydroxamic acid (—), all 0.57 mM in 50% EtOH/ $\text{H}_2\text{O}$  containing 0.19 mM  $\text{FeCl}_3$ .

underlines the limitations of these “hydroxamate analogues”, as they may not possess hydroxamate-like binding properties.

**Single-Crystal X-ray Structure of **5b** and **6c**.** The single-crystal X-ray structures of the hydroxamate ester **5b** and amide **6c** were determined. The structures prove the connectivity of the squarate hydroxamates. However, the conformations of both compounds are of note. Instead of the initially expected intramolecular H-bond between the *N*-OH group and an adjacent carbonyl group of the putative metal binding site, the compounds form an intermolecular H-bond in the crystal. The ball-and-stick

(29) Konetschny-Rapp, S.; Jung, G.; Raymond, K. N.; Meiwes, J.; Zähler, H. *J. Am. Chem. Soc.* **1992**, *114*, 2224–2230.



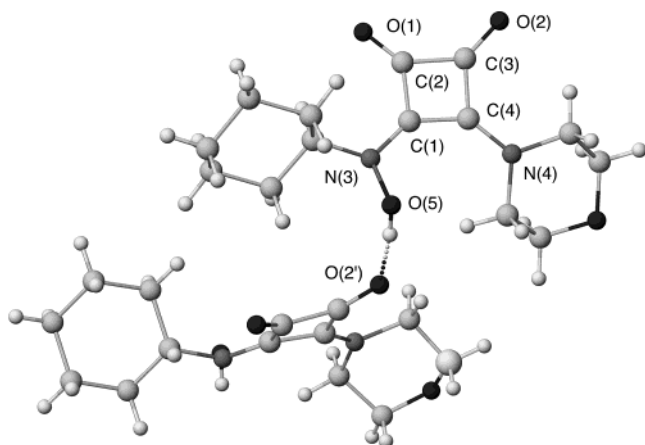


**FIGURE 3.** Ball-and-stick representation and numbering scheme used for a H-bonded dimer found in the solid-state structure of **6c**; temperature of data collection = 198 K. Selected bond distances: C(1)–C(2) = 1.470(2) Å, C(2)–C(3) = 1.489(2) Å, C(3)–C(4) = 1.466(2) Å; C(4)–C(1) = 1.415(2) Å, C(2)–O(1) = 1.214(2) Å, C(3)–O(2) = 1.232(2) Å, C(1)–N(3) = 1.333(2) Å, N(3)–O(5) = 1.413(2) Å, C(4)–N(4) = 1.326(2) Å, O(5)–O(2') = 2.657(2) Å; N(3)–O(5)–O(2') angle = 99.4°; rms of cyclobutenedione framework = 0.059 Å.

model showing one H-bond expressed by hydroxyl amide squarate **6c** in the solid state is shown in Figure 3.

In light of the deduced electronic and observed metal binding differences between the ester and the amide hydroxamates, the observed conformation may not be entirely unexpected for the hydroxamate ester **5b**, but it is certainly unexpected for the hydroxamate amide **6c**. Nonetheless, much of the spectroscopic differences between the esters and the amides can also be seen in the crystal structures. For instance, through comparison of the relative trends in the bond lengths of equivalent bond distances found in **5b** and **6c**, the differing electronic influences of the ester and amide functionality on the electron-density (or bond order) of the carbonyl oxygen adjacent to the *N*-hydroxylamide functionality can be traced. They are predicted on the basis of the spectroscopic evidence. The two carbonyl C–O bond distances in the hydroxamate ester **5b** (1.178 and 1.209 Å) are much shorter than the two carbonyl C–O bond distances in the hydroxamate amide **6c** (1.214 and 1.232 Å). In either case, the longer of the two bond lengths is found for the C–O bond diagonally across the hydroxamate moiety, providing evidence for the strongly electron-donating nature of the *N*-OH moiety. The large difference between the two bond lengths in the ester versus the relatively equal bond distances in the amide highlights the electronic difference between the ester and the amide moiety. The C–C bond length differences observed in these compounds also parallel the inferred resonance pathways. Thus, the crystal structures confirm the spectroscopically derived conclusions and provide a structural explanation for the differing metal binding properties of these compounds.

The structures further highlight the fundamental differences between hydroxamate squarates and hydroxamic acids, although the existence of intermolecular H-bonds in **5b** or **6c** in solution cannot be excluded. The molecules are arranged in the lattice in an extensive network of intermolecular H-bonds but it cannot be

excluded that the observation of the intermolecular H-bonds are a crystal packing effect.

## Conclusion

In conclusion, squarate hydroxamate esters **5** and hydroxamate amides **6** were prepared and fully characterized. While esters **5** do not bind iron(III) in aqueous systems, amides **6** do. The difference in their coordination behavior can be rationalized on the basis of the variation of the resonance stabilization of these molecules. The dominating resonance structures also determine the mechanism of formation of the squarate hydroxamates. An investigation of the spin–lattice relaxation time  $T_1$  of a range of derivatives allowed us to define guidelines for the reliable NMR spectroscopic characterization of squarate derivatives. The spectroscopically derived conclusions regarding the prevailing resonance structures in these molecules were also seen in the solid-state structure of the hydroxamate ester and the amide. In all, the hydroxamate squarates differ in key properties from hydroxamic acids.

A metal coordinated to the *O,O*-chelate of the hydroxamic acid-like moiety of the hydroxamate amides **6** is electronically coupled with the amide nitrogen on the opposite side. This coupling makes them attractive platforms for the synthesis of molecular chemosensors. Thus, the understanding of the bond arrangements controlling the metal binding in these novel iron(III)-chelating moieties forms the basis for their use in the construction of molecular sensors, a goal we are currently pursuing.<sup>31</sup>

## Experimental Section

**WARNING.** Liquid, lipophilic squaric acid diesters are known to be potent topical allergens.<sup>8</sup> Two of us contracted a contact dermatitis on exposed areas on hands, arms, and face that required medical attention after having worked with solid amide esters such as **3** (exposure through dusts generated while scraping the compounds from a round-bottom flask) and during the preparation of diethylsquarate from halogenated intermediates.<sup>3,32</sup> We did not experience any problems when working with the *N*-hydroxylamide derivatives. However, we did not test the compounds and habitually exercised caution when working with these compounds (gloves, transfer of solids only under a well-ventilated fumehood).

**Materials.** 3,4-Dimethoxycyclobut-3-ene-1,2-dione (**2a**, dimethyl squarate),  $R_f = 0.89$  (silica–CH<sub>3</sub>CN),<sup>21</sup> 3-methoxy-4-*N*-diethylaminocyclobut-3-ene-1,2-dione (**3a**),<sup>22</sup> 3,4-bis(diethylamino)cyclobut-3-ene-1,2-dione (**4a**),<sup>23</sup> and 3,4-bis(dibenzylamino)cyclobut-3-ene-1,2-dione (**4c**)<sup>23</sup> were prepared according to literature procedures. Spectroscopic and analytical data for the known compounds are provided for comparison and because some data differ from literature-reported data and no <sup>13</sup>C NMR data were reported for any of these compounds.

**3-Methoxy-4-*N*-morpholinylcyclobut-3-ene-1,2-dione (3b).** 3,4-Dimethoxycyclobut-3-ene-1,2-dione (**2a**) (500 mg, 3.52 mmol) was dissolved in MeOH (4 mL), and morpholine (307 μL, 3.52 mmol) was added; the mixture was heated to reflux. The formation of a white precipitate was observed. Once all

(30) Detailed description of the H-bond networks expressed by these and related compounds will be reported in a separate manuscript.

(31) Lim, N. C.; Yao, L.; Freake, H. C.; Brückner, C. *Abstract of Papers*, 225th National Meeting of the American Chemical Society, New Orleans, LA, Mar. 27–23, 2003; American Chemical Society: Washington, DC, 2003; INORG 884.

(32) Maahs, G. *Angew. Chem., Int. Ed. Engl.* **1963**, *2*, 690–691.

the starting material was consumed (after 36 h, TLC control), Et<sub>2</sub>O (1 mL) was added to the hot solution, which then was cooled to 0 °C. Crystals were formed overnight and filtered off using a glass frit (M). Washing of the filter cake with cold Et<sub>2</sub>O and drying under vacuum at ambient temperature afforded **3b** (0.52 g, 75% yield) as analytically pure white crystals: *R<sub>f</sub>* = 0.29 (silica-CH<sub>2</sub>Cl<sub>2</sub>/20% CH<sub>3</sub>CN); mp = 152–154 °C (uncorrected); <sup>1</sup>H NMR (DMSO-*d*<sub>6</sub>, 400 MHz, 75 °C,  $\delta$ ) 4.29 (s, 3H), 3.72–3.70 (m, 8H) ppm; <sup>13</sup>C NMR (DMSO-*d*<sub>6</sub>, 100 MHz, D1 = 5 s, 75 °C,  $\delta$ ) 189.3, 182.5, 177.0, 170.3, 66.3, 60.8, 47.2 ppm; IR (KBr)  $\nu_{\text{max}}$  1798 (w, C=O), 1705 (m, C=O), 1627 (s), 1496 (m), 1407 (m), 1277 (m), 1110 (m) cm<sup>-1</sup>; MS (FAB+, NBA) *m/z* 198 (MH<sup>+</sup>, 76%); HR-MS (FAB+ of MH<sup>+</sup>, NBA) *m/z* calcd for C<sub>9</sub>H<sub>12</sub>NO<sub>4</sub> 198.0766, found 198.0746.

**3-Benzylamino-4-methoxycyclobut-3-ene-1,2-dione (3c).** 3,4-Dimethoxycyclobut-3-ene-1,2-dione (**2a**) (4.0 g, 28.1 mmol) was dissolved in MeOH (100 mL). Benzylamine (3.25 mL, 29.2 mmol) was added, and the mixture was stirred at ambient temperature for ~1 h. The solution was then taken to dryness by rotary evaporation. Column chromatography (silica-20% CH<sub>3</sub>CN/CH<sub>2</sub>Cl<sub>2</sub>) was used to isolate and purify **3c** as a white solid (5.1 g, 83% yield): *R<sub>f</sub>* = 0.60 (silica-CH<sub>2</sub>Cl<sub>2</sub>/20% CH<sub>3</sub>CN); mp = 122–124 °C (uncorrected); <sup>1</sup>H NMR (DMSO-*d*<sub>6</sub>, 400 MHz,  $\delta$ ) 7.38–7.29 (m, 5H), 4.67 (s, 1H), 4.56 (s, 1H), 4.29 (s, 3H) ppm; <sup>13</sup>C NMR (DMSO-*d*<sub>6</sub>, 100 MHz,  $\delta$ ) 189.8, 183.3, 178.0, 173.1, 138.7, 129.0, 127.9, 127.8, 60.3, 47.8 ppm; IR (KBr)  $\nu_{\text{max}}$  3206 (br, NH), 2952 (m), 2925 (m), 1795 (s, C=O), 1705 (s, C=O), 1594 (s), 1508 (s), 1435 (s), 1408 (s), 1355 (s), 1049 (m), 921 (s), 831 (m), 741 (s), 693 (s) cm<sup>-1</sup>; MS (ES+, 100% CH<sub>3</sub>CN, 30 V) *m/z* = 240 (MNa<sup>+</sup>); MS (FAB+, NBA) *m/z* = 218 (MH<sup>+</sup>, 51%); HR-MS (FAB+ of MH<sup>+</sup>, NBA) *m/z* calcd for C<sub>12</sub>H<sub>12</sub>NO<sub>3</sub> 218.0817, found 218.0809.

**3-Diethylamino-4-morpholinocyclobut-3-ene-1,2-dione (4b).** Squarate amide ester **3a** (228 mg, 1.24 mmol) was dissolved in EtOH (6 mL) and reacted with morpholine (1.63 mL, 18.7 mmol) under reflux conditions. Upon consumption of **3a** as monitored by TLC (~24 h), the solution was evaporated in vacuo to yield a yellow solid residue. This solid was recrystallized from hot, anhydrous EtOH, to yield light yellow crystals of **4b** (0.28 g, 94% yield): *R<sub>f</sub>* = 0.50 (silica-CH<sub>3</sub>CN); mp = 102 °C (uncorrected); <sup>1</sup>H NMR (DMSO-*d*<sub>6</sub>, 400 MHz,  $\delta$ ) 3.69 (br t, *J* = 5.0 Hz, 4H), 3.59 (br t, *J* = 5.0 Hz, 4H), 3.51 (q, *J* = 7.2 Hz, 4H), 1.16 (t, *J* = 7.2 Hz, 6H) ppm; <sup>13</sup>C NMR (DMSO-*d*<sub>6</sub>, 100 MHz,  $\delta$ ) 183.9, 183.1, 168.6, 167.5, 66.1, 48.3, 43.9, 13.8 ppm; IR (KBr)  $\nu_{\text{max}}$  3427 (br), 2969 (m), 2926 (m), 2869 (m), 1778 (s, C=O), 1663 (s, C=O), 1590 (s), 1519 (s), 1455 (s), 1305 (m), 1274 (s), 1218 (m), 1167 (m), 1112 (s), 1065 (m), 1023 (m), 991 (m), 883 (m), 789 (m) cm<sup>-1</sup>; MS (ES+, 100% CH<sub>3</sub>CN, 30 V) *m/z* = 261 (MNa<sup>+</sup>); MS (FAB+, NBA) *m/z* = 239 (MH<sup>+</sup>, 96%); HR-MS (FAB+ of MH<sup>+</sup>, NBA) *m/z* calcd for C<sub>12</sub>H<sub>19</sub>N<sub>2</sub>O<sub>3</sub> 239.1396, found 239.1400.

**3-Benzylamino-4-diethylaminocyclobut-3-ene-1,2-dione (4d).** Squarate amide ester **3c** (220 mg, 1.0 mmol) was dissolved in EtOH (4 mL) and reacted with diethylamine (1.6 mL, 15.5 mmol) under reflux conditions for 5 min. Workup was performed as described for **3b** (Et<sub>2</sub>O, 3 mL). The dried white crystals formed were analytically pure (0.26 g, 99% yield): *R<sub>f</sub>* = 0.24 (silica-20% CH<sub>3</sub>CN/CH<sub>2</sub>Cl<sub>2</sub>); mp = 175–177 °C (uncorrected); <sup>1</sup>H NMR (DMSO-*d*<sub>6</sub>, 400 MHz,  $\delta$ ) 7.38–7.27 (m, 5H), 4.78 (s, 2H), 3.54 (br s, 4H), 1.13 (t, *J* = 7.1 Hz, 6H); <sup>13</sup>C NMR (DMSO-*d*<sub>6</sub>, 100 MHz, D1 = 4 s, LB = 5 Hz,  $\delta$ ) 183.0, 182.2, 167.4, 167.0, 140.0, 128.9, 127.8, 127.6, 46.9, 43.9, 15.5 ppm; IR (KBr)  $\nu_{\text{max}}$  3203 (br, NH), 2966 (m), 1789 (m, C=O), 1659 (s, C=O), 1570 (s), 1528 (s), 1443 (s), 1315 (m), 1075 (m), 696 (m) cm<sup>-1</sup>; MS (FAB+, NBA) *m/z* = 258 (M<sup>+</sup>, 88%), 259 (MH<sup>+</sup>, 99%); HR-MS (FAB+ of MH<sup>+</sup>, NBA) *m/z* calcd for C<sub>15</sub>H<sub>19</sub>N<sub>2</sub>O<sub>2</sub> 259.1447, found 259.1437.

**3-Methoxy-4-N-methylhydroxylaminocyclobut-3-ene-1,2-dione (5a).** 3,4-Dimethoxy-3-cyclobutene-1,2-dione (**2a**) (7.0 g, 49.3 mmol) was dissolved in MeOH (60 mL), and a slight excess of *N*-methylhydroxylamine hydrochloride (4.62 g, 55.3 mmol) was added. Upon addition of KOH (3.35 g, 59.7 mmol),

a white precipitate resulted. Stirring at ambient temperature was continued for ~1 h (monitored by TLC). The mixture was then filtered; the filter cake was washed with cold MeOH, and the combined filtrates were taken to dryness by rotary evaporation. Purification of **5a** was achieved by column chromatography (silica-20% CH<sub>3</sub>CN/CH<sub>2</sub>Cl<sub>2</sub>) to yield a white solid (4.9 g, 63% yield): *R<sub>f</sub>* = 0.45 (silica-20% CH<sub>3</sub>CN/CH<sub>2</sub>Cl<sub>2</sub>); mp = 135–140 °C dec (uncorrected) (lit. 177–178 °C);<sup>20</sup> <sup>1</sup>H NMR (DMSO-*d*<sub>6</sub>, 400 MHz,  $\delta$ ) 4.28 (s, 3H), 3.38 (s, 3H) ppm; <sup>13</sup>C NMR (DMSO-*d*<sub>6</sub>, 100 MHz, D1 = 5 s, LB = 5 Hz,  $\delta$ ) 185.2, 179.3, 174.5, 167.8, 60.3, 40.7 ppm; IR (KBr)  $\nu_{\text{max}}$  3087 (br), 2796 (br, OH), 1806 (s, C=O), 1709 (s, C=O), 1626 (s), 1508 (m), 1489 (m), 1450 (m), 1390 (s), 1257 (m), 1202 (s), 1166 (s), 1122 (m), 1074 (s), 1040 (m), 944 (s), 885 (m), 834 (s), 782 (m), 769 (m) cm<sup>-1</sup>; MS (ES-) *m/z* = 156 (M<sup>-</sup>); MS (FAB+, NBA) *m/z* = 158 (MH<sup>+</sup>, 83%); HR-MS (FAB+ of MH<sup>+</sup>, NBA) *m/z* calcd for C<sub>6</sub>H<sub>8</sub>NO<sub>4</sub> 158.0453, found 158.0448. Anal. Calcd for C<sub>6</sub>H<sub>7</sub>NO<sub>4</sub>: C, 45.86; H, 4.49; N, 8.91. Found: C, 45.92; H, 4.60; N, 9.11.

**3-Methoxy-4-N-isopropylhydroxylaminocyclobut-3-ene-1,2-dione (5b).** Prepared as a white solid according to the procedure described for **5a** (92% yield, 3.59 g): *R<sub>f</sub>* = 0.65 (silica-40% CH<sub>3</sub>CN/CH<sub>2</sub>Cl<sub>2</sub>); mp = 148–150 °C dec (uncorrected) (lit. 141–142 °C);<sup>20</sup> <sup>1</sup>H NMR (DMSO-*d*<sub>6</sub>, 400 MHz,  $\delta$ ) 10.53 (br s, 1H), 4.34 (br s, 1H), 4.29 (s, 3H), 1.19 (d, *J* = 6.6 Hz, 6H) ppm; <sup>13</sup>C NMR (DMSO-*d*<sub>6</sub>, 100 MHz, D1 = 5 s, LB = 5 Hz,  $\delta$ ) 185.4, 179.5, 175.0, 167.7, 60.3, 53.5, 19.2 ppm; IR (KBr)  $\nu_{\text{max}}$  3096 (br), 2823 (br, OH), 1796 (s, C=O), 1710 (s, C=O), 1602 (s), 0.1496 (s), 1467 (s), 1402 (s), 1367 (s), 1193 (s), 1173 (s), 1122 (s), 1052 (s), 1028 (s), 941 (s), 904 (s), 850 (s), 752 (s) cm<sup>-1</sup>; MS (ES-, 100% CH<sub>3</sub>CN, 30 V) *m/z* = 184 (M<sup>-</sup>); MS (FAB+, NBA) *m/z* = 186 (MH<sup>+</sup>, 100%); HR-MS (FAB+ of MH<sup>+</sup>, NBA) *m/z* calcd for C<sub>8</sub>H<sub>12</sub>NO<sub>4</sub> 186.0766, found 186.0743. Anal. Calcd for C<sub>8</sub>H<sub>11</sub>NO<sub>4</sub>: C, 51.89; H, 5.99; N, 7.56. Found: C, 51.59; H, 5.61; N, 7.92.

**3-Methoxy-4-N-cyclohexylhydroxylaminocyclobut-3-ene-1,2-dione (5c).** Prepared as a white solid from **2a** and cyclohexylhydroxylamine according to the procedure described for **5a** (2.56 g, 81% yield): *R<sub>f</sub>* = 0.77 (silica-20% CH<sub>3</sub>CN/CH<sub>2</sub>Cl<sub>2</sub>); mp = 158–159 °C dec (uncorrected) (lit. 149–151 °C);<sup>20</sup> <sup>1</sup>H NMR (DMSO-*d*<sub>6</sub>, 400 MHz,  $\delta$ ) 10.56 (br s, 1H), 4.29 (s, 3H), 3.93 (br s, 1H), 1.79–1.06 (m, 10H) ppm; <sup>13</sup>C NMR (DMSO-*d*<sub>6</sub>, 100 MHz, D1 = 3 s, LB = 5 Hz,  $\delta$ ) 186.0, 180.1, 175.7, 168.3, 61.8, 60.9, 29.8, 25.1, 25.0 ppm; IR (KBr)  $\nu_{\text{max}}$  2933 (s), 2856 (m, OH), 1787 (m, C=O), 1695 (m, C=O), 1637 (s), 1495 (s), 1381 (s), 1058 (m), 760 (m) cm<sup>-1</sup>; MS (ES-, 100% CH<sub>3</sub>CN, 30 V) *m/z* = 224 (M<sup>-</sup>); MS (FAB+, NBA) *m/z* = 226 (MH<sup>+</sup>, 28%), 264 (MK<sup>+</sup>, 99%), 302 (M - H<sup>+</sup>·2K<sup>+</sup>, 66%); HR-MS (FAB+ of MH<sup>+</sup>, NBA) *m/z* calcd for C<sub>11</sub>H<sub>16</sub>NO<sub>4</sub> 226.1079, found 226.1059.

**3-Morpholino-4-N-methylhydroxylaminocyclobut-3-ene-1,2-dione (6a).** Squarate hydroxamate ester **5a** (600 mg, 3.8 mmol) was dissolved in MeOH and titrated with morpholine at ambient temperature (TLC control). Once all the starting material was consumed, the solution was taken to dryness by rotary evaporation yielding a yellow residue that was recrystallized from hot water yielding **6a** as a white solid (0.50 g, 62% yield): *R<sub>f</sub>* = 0.23 (silica-CH<sub>3</sub>CN); mp = 128–130 °C dec (uncorrected); <sup>1</sup>H NMR (DMSO-*d*<sub>6</sub>, 400 MHz,  $\delta$ ) 10.91 (br s, 1H), 3.85 (t, *J* = 4.5 Hz, 4H), 3.68 (t, *J* = 4.4, 4H), 3.47 (s, 3H) ppm; <sup>13</sup>C NMR (DMSO-*d*<sub>6</sub>, 100 MHz, D1 = 5 s,  $\delta$ ) 180.5, 178.6, 165.1, 164.4, 66.0, 48.7, 41.2 ppm; IR (KBr)  $\nu_{\text{max}}$  3413 (br), 2662 (br, OH), 1783 (s, C=O), 1660 (s, C=O), 1588 (s), 1445 (s), 1406 (s), 1310 (s), 1292 (s), 1205 (s), 1109 (s), 1025 (s), 867 (m) cm<sup>-1</sup>; MS (ES+, 100% CH<sub>3</sub>OH, 30 V) *m/z* = 235 (MNa<sup>+</sup>); MS (FAB+, NBA) *m/z* = 212 (M<sup>+</sup>, 42%), 213 (MH<sup>+</sup>, 76%), 235 (MNa<sup>+</sup>, 15%); HR-MS (FAB+ of MH<sup>+</sup>, NBA) *m/z* calcd for C<sub>9</sub>H<sub>13</sub>N<sub>2</sub>O<sub>4</sub> 213.0875, found 213.0855. Anal. Calcd for C<sub>9</sub>H<sub>12</sub>N<sub>2</sub>O<sub>4</sub>: C, 50.94; H, 5.70; N, 13.20. Found: C, 50.76; H, 6.01; N, 13.26.

**3-Morpholino-4-N-isopropylhydroxylaminocyclobut-3-ene-1,2-dione (6b).** Prepared in 67% yield (131 mg) from **5b** and morpholine as described for **6a**: *R<sub>f</sub>* = 0.43 (silica-CH<sub>3</sub>CN); mp = 148–150 °C dec (uncorrected); <sup>1</sup>H NMR (DMSO-



$\delta$ ) 10.28 (br s, 1H), 4.66 (heptet,  $J = 6.5$  Hz, 1H), 3.86 (t,  $J = 4.5$ , 4H), 3.69 (t,  $J = 4.5$  Hz, 4H), 1.18 (d,  $J = 6.5$  Hz, 6H) ppm;  $^{13}\text{C}$  NMR (DMSO- $d_6$ , 100 MHz, D1 = 5 s,  $\delta$ ) 180.8, 178.7, 165.7, 164.7, 66.0, 53.4, 48.7, 19.2 ppm; IR (KBr)  $\nu_{\text{max}}$  3435 (br, OH), 1779 (s, C=O), 1662 (s, C=O), 1585 (s), 1497 (s), 1445 (s), 1364 (m), 1308 (s), 1281 (s), 1190 (s), 1121 (s), 1023 (m), 1006 (m), 883 (m), 826 (m)  $\text{cm}^{-1}$ ; MS (ES+, 100%  $\text{CH}_3\text{OH}$ , 30 V)  $m/z = 263$  ( $\text{M}^+$ ); MS (FAB+, NBA)  $m/z = 240$  ( $\text{M}^+$ , 41%), 241 ( $\text{MH}^+$ , 74%); HR-MS (FAB+ of  $\text{MH}^+$ , NBA)  $m/z$  calcd for  $\text{C}_{11}\text{H}_{17}\text{N}_2\text{O}_4$  241.1188, found 241.1178. Anal. Calcd for  $\text{C}_{11}\text{H}_{16}\text{N}_2\text{O}_4$ ; C, 54.99; H, 6.71; N, 11.66. Found: C, 54.99; H, 6.47; N, 11.90.

**3-Morpholino-4-*N*-cyclohexylhydroxylaminocyclobut-3-ene-1,2-dione (6c).** Prepared in 71% yield (360 mg) from **5c** and morpholine as described for **6a**:  $R_f = 0.29$  (silica gel- $\text{CH}_3\text{CN}$ ); mp = 167–169 °C dec (uncorrected);  $^1\text{H}$  NMR (DMSO- $d_6$ , 400 MHz,  $\delta$ ) 10.35 (br s, 1H), 4.23 (m, 1H), 3.85 (t,  $J = 4.4$  Hz, 4H), 3.68 (t,  $J = 4.4$  Hz, 4H), 1.79–1.25 (m, 10H) ppm;  $^{13}\text{C}$  NMR (DMSO- $d_6$ , 100 MHz, D1 = 10 s, LB = 5 Hz,  $\delta$ ) 180.8, 178.7, 165.7, 164.7, 66.1, 60.9, 48.7, 29.3, 24.8 (2 overlapping signals) ppm; IR (KBr)  $\nu_{\text{max}}$  3119 (br), 2928 (m), 2855 (m, OH), 1784 (m, C=O), 1672 (s, C=O), 1575 (s), 1492 (s), 1442 (s), 1280 (s), 1116 (m)  $\text{cm}^{-1}$ ; MS (ES-, 100%  $\text{CH}_3\text{CN}$ , 30 V)  $m/z = 279$  ( $\text{M}^-$ ); MS (FAB+, NBA)  $m/z = 280$  ( $\text{M}^+$ , 40%), 281 ( $\text{MH}^+$ , 65%); HR-MS (FAB+ of  $\text{M}^+$ , NBA)  $m/z$  calcd for  $\text{C}_{14}\text{H}_{21}\text{N}_2\text{O}_4$  281.1501, found 281.1497. Anal. Calcd for  $\text{C}_{14}\text{H}_{20}\text{N}_2\text{O}_4$ ; C, 59.99; H, 7.19; N, 9.99. Found: C, 59.63; H, 7.62; N, 10.11.

**3-Methoxy-4-*N*,*O*-dimethylaminocyclobut-3-ene-1,2-dione (9a).** 3,4-Dimethoxycyclobut-3-ene-1,2-dione (**2a**) (620 mg, 4.36 mmol) was dissolved in MeOH (2.5 mL) and free base *N*,*O*-dimethylamine (1.7 equiv, 11.0 mL of a solution 0.7 M in MeOH) was added. The methanolic free base *N*,*O*-dimethylamine solution was prepared by addition of a methanolic KOH solution (0.43 g in 4 mL MeOH) to a solution of *N*,*O*-dimethylammonium hydrochloride in MeOH (0.75 g in 7 mL MeOH), followed by filtration of the precipitated KCl. The reaction mixture was stirred at ambient temperature until all starting material was consumed (~1 h, monitored by TLC). The solvent was removed, and the resulting yellow residue was taken up in hot methanol and then cooled to 0 °C. Crystals were formed and filtered off using a glass frit (M). The yellow crystals were washed with cold petroleum ether 30–60 and dried under vacuum at ambient temperature to afford **9a** (0.68 g, 91% yield) as yellowish crystals:  $R_f = 0.37$  (silica- $\text{CH}_2\text{Cl}_2$ ); mp = 112–114 °C (uncorrected) (lit. 101–103 °C);  $^{20}\text{H}$  NMR (DMSO- $d_6$ , 400 MHz,  $\delta$ ) 4.31 (s, 3H), 3.75 (s, 3H), 3.38 (s, 3H) ppm;  $^{13}\text{C}$  NMR (DMSO- $d_6$ , 100 MHz,  $\delta$ ) 185.3, 180.9, 175.9, 169.0, 62.7, 61.2, 37.8 ppm; IR (KBr)  $\nu_{\text{max}}$  1799 (m, C=O), 1715 (s, C=O), 1625 (s), 1497 (s), 1398 (s)  $\text{cm}^{-1}$ ; MS (FAB+, NBA)  $m/z$  171 ( $\text{M}^+$ , 27%), 172 ( $\text{MH}^+$ , 100%), 210 ( $\text{MK}^+$ , 15%); HR-MS (FAB+ of  $\text{M}^+$ , NBA)  $m/z$  calcd for  $\text{C}_7\text{H}_{10}\text{NO}_4$  172.0610, found 172.0610.

**3-Methoxy-4-methoxyaminocyclobut-3-ene-1,2-dione (9b).** 3,4-Dimethoxycyclobut-3-ene-1,2-dione (**2a**) (530 mg, 3.73 mmol) was dissolved in MeOH (3.5 mL) and free base methoxyamine (3.0 mL of a solution 1.25 M in MeOH, prepared as described for **9a** from 0.21 g KOH in 1 mL of MeOH and 0.31 g methoxyammonium hydrochloride in 2 mL of MeOH) was added. The mixture was stirred at ambient temperature until all starting material was consumed (~24 h, monitored by TLC). The solution was taken to dryness by rotary evaporation. Column chromatography (silica- $\text{CH}_2\text{Cl}_2$ ) was used to isolate and purify **9b** as a white solid (120 mg, 20% yield):  $R_f = 0.24$  (silica- $\text{CH}_2\text{Cl}_2$ /20%  $\text{CH}_3\text{CN}$ ); mp = 110–112 °C (uncorrected) (lit. 103–104 °C);  $^{20}\text{H}$  NMR (DMSO- $d_6$ , 400 MHz,  $\delta$ ) 4.28 (s, 3H), 3.70 (s, 3H) ppm;  $^{13}\text{C}$  NMR spectrum could not be recorded because the compound decomposed over the course of 12 h in DMSO- $d_6$ ; IR (KBr)  $\nu_{\text{max}}$  3167 (br, NH), 1803 (m, C=O), 1703 (s, C=O), 1613 (s), 1514 (m), 1371 (s), 1011 (m), 938 (m)  $\text{cm}^{-1}$ ; MS (ES-, 100%  $\text{CH}_3\text{CN}$ , 30 V)  $m/z = 156$  ( $\text{M}^-$ ); MS (FAB+, NBA)  $m/z = 158$  ( $\text{MH}^+$ , 100%); HR-MS (FAB+ of  $\text{M}^+$ , NBA)  $m/z$  calcd for  $\text{C}_6\text{H}_8\text{NO}_4$  158.0453, found 158.0456.

**3-Morpholino-4-*N*,*O*-dimethylaminocyclobut-3-ene-1,2-dione (10).** Squarate ester hydroxamate **9a** (160 mg, 0.94 mmol) was dissolved in MeOH (5 mL), and morpholine (0.5 mL, 5.7 mmol) was added at ambient temperature. Once all the starting material was consumed (TLC control) and a white precipitate had formed, the product was filtered off, yielding **10** as white solid (130 mg, 62% yield):  $R_f = 0.74$  (silica- $\text{CH}_3\text{CN}$ ); mp = 161–162 °C dec (uncorrected);  $^1\text{H}$  NMR (DMSO- $d_6$ , 400 MHz,  $\delta$ ) 3.80 (t,  $J = 4.3$  Hz, 4H), 3.72–3.69 (m, 7H), 3.44 (s, 3H) ppm;  $^{13}\text{C}$  NMR (DMSO- $d_6$ , 100 MHz,  $\delta$ ) 182.4, 179.3, 166.7, 164.4, 66.5, 60.2, 48.9, 37.7 ppm; IR (KBr)  $\nu_{\text{max}}$  1785 (m, C=O), 1675 (s, C=O), 1601 (s), 1499 (s), 1287 (m), 1107 (m)  $\text{cm}^{-1}$ ; MS (ES+, 100%  $\text{CH}_3\text{CN}$ , 30 V)  $m/z = 227$  ( $\text{M}^+$ ); MS (FAB+, NBA)  $m/z = 226$  ( $\text{M}^+$ , 22%), 227 ( $\text{MH}^+$ , 35%), 265 ( $\text{MK}^+$ , 5%); HR-MS (FAB+ of  $\text{M}^+$ , NBA)  $m/z$  calcd for  $\text{C}_{10}\text{H}_{15}\text{N}_2\text{O}_4$  227.1037, found 227.1030.

**3-Hydroxy-4-*N*-isopropylaminocyclobut-3-ene-1,2-dione (11b).** Squarate ester hydroxamate **5b** (160 mg, 0.86 mmol) was dissolved in aq HCl (3.6%, 10 mL) and stirred at ambient temperature. Once all the starting material was consumed (TLC control, ~2 days), the solution was taken to dryness by rotary evaporation, yielding a yellowish residue. The residue was taken up in aq HCl (1M, 10 mL) and extracted with ether (3  $\times$  20 mL). Isolation of the organic phase and evaporation of solvent afforded the hydrolyzed product **11b** (0.10 g, 70% yield): mp = 233–235 °C dec (uncorrected);  $^1\text{H}$  NMR (DMSO- $d_6$ , 400 MHz,  $\delta$ ) 8.35 (d,  $J = 7.6$  Hz, 1H), 3.94 (m, 1H), 1.14 (t,  $J = 7.2$  Hz, 6H) ppm;  $^{13}\text{C}$  NMR (DMSO- $d_6$ , 100 MHz, D1 = 14 s, LB = 5 Hz,  $\delta$ ) 187.0 (v br), 186.1, 184.7 (v br), 174.8, 47.9, 25.1 ppm; IR (KBr)  $\nu_{\text{max}}$  3225 (br), 2979 (br), 2638 (br), 1818 (m), 1689 (s, C=O), 1628 (s, C=O), 1535 (s), 1464 (s), 1425 (s), 1337 (s), 1127 (m)  $\text{cm}^{-1}$ ; MS (ES+, 100%  $\text{CH}_3\text{CN}$ , 30 V)  $m/z = 156$  ( $\text{MH}^+$ ). Anal. Calcd for  $\text{C}_7\text{H}_9\text{NO}_3$ ; C, 54.19; H, 5.85; N, 9.03. Found: C, 53.80; H, 5.61; N, 9.14.

**3-Hydroxy-4-*N*-cyclohexylhydroxylaminocyclobut-3-ene-1,2-dione (11c).** Prepared in 60% yield (110 mg, 0.56 mmol) from **5c** and aq HCl (3.6%, 10 mL) as described for **11b**: mp = 233–235 °C dec (uncorrected);  $^1\text{H}$  NMR (DMSO- $d_6$ , 400 MHz,  $\delta$ ) 8.38 (d,  $J = 7.7$  Hz, 1H), 3.6 (s, 1H), 1.81–1.04 (m, 10H) ppm;  $^{13}\text{C}$  NMR (DMSO- $d_6$ , 100 MHz, D1 = 10 s,  $\delta$ ) 187.0 (v br), 186.2, 184.7 (v br), 174.9, 55.0, 35.3, 26.8, 26.4 ppm; IR (KBr)  $\nu_{\text{max}}$  3248 (br), 2932 (br), 2659 (br), 1818 (m), 1677 (br, s), 1534 (s), 1426 (s), 1365 (m), 1092 (m), 803 (m)  $\text{cm}^{-1}$ ; MS (ES+, 100%  $\text{CH}_3\text{CN}$ , 30 V)  $m/z = 196$  ( $\text{MH}^+$ ). Anal. Calcd for  $\text{C}_{10}\text{H}_{13}\text{NO}_3$ ; C, 61.53; H, 6.71; N, 7.17. Found: C, 61.22; H, 6.94; N, 6.95.

**3-Hydroxy-4-*N*-benzylaminocyclobut-3-ene-1,2-dione (11d).** Prepared in 96% yield from **3c** and aq HCl (3.6%, 10 mL) as described for **11b** (0.9 mmol scale): mp = 205–210 °C dec (uncorrected);  $^1\text{H}$  NMR (DMSO- $d_6$ , 400 MHz,  $\delta$ ) 8.83 (s, 1H), 7.35 (m, 5H), 4.58 (d,  $J = 6.2$  Hz, 2H) ppm;  $^{13}\text{C}$  NMR (DMSO- $d_6$ , 100 MHz, D1 = 10 s,  $\delta$ ) 184.7 (v br peak overlapping sharp signal), 183.8 (v br), 173.7, 138.6, 128.5, 127.5, 46.9, 15.1 ppm; IR (KBr)  $\nu_{\text{max}}$  3260 (br), 1810 (m), 1680 (s), 1567 (s), 1510 (s), 1341 (m), 1261 (m), 1082 (m), 912 (m), 694 (m)  $\text{cm}^{-1}$ ; MS (ES+, 100%  $\text{CH}_3\text{CN}$ , 30V)  $m/z = 204$  ( $\text{MH}^+$ ); MS (ES-, 100%  $\text{CH}_3\text{CN}$ , 30V)  $m/z = 202$  ( $\text{M}^-$ ).

**Acknowledgment.** We thank the donors of the Petroleum Research Fund (PRF), administered by the American Chemical Society (ACS), the Research Foundation at the University of Connecticut (C.B. and N.L.), and Saint Mary's University (H.J.) for financial support. We thank Andreas Decken, University of New Brunswick, for diffraction data collection for **6c**.

**Supporting Information Available:**  $^{13}\text{C}$  and  $^1\text{H}$  NMR spectra of **5a–c**, **6a–c**, and **11b–d** and details of the X-ray crystallographic determination (tabulated crystal data, ORTEPS, and a CIF file) of **5b** and **6c**. This material is available free of charge via the Internet at <http://pubs.acs.org>.

JO035175G